Flügge's Conjecture: Dissipation-versus Deflection-Induced Pavement–Vehicle Interactions

Article *in* Journal of Engineering Mechanics · November 2013

DOI: 10.1061/(ASCE)EM.1943-7889.0000754

3 authors, including:

Arghavan Louhghalam
University of Massachusetts Dartmouth
18 PUBLICATIONS **85** CITATIONS

SEE PROFILE

Flügge's Conjecture: Dissipation vs. Deflection Induced Pavement–Vehicle–Interactions (PVI)

Arghavan Louhghalam,[1] Member, ASCE

Mehdi Akbarian,[2] Member, ASCE

Franz-Josef Ulm,[3] Member, ASCE

[1]Postdoctoral Researcher, Department of Civil & Environmental Engineering, Massachusetts Institute of Technology, Cambridge MA 02139, Email: arghavan@mit.edu

[2]Graduate Research Assistant, Department of Civil & Environmental Engineering, Massachusetts Institute of Technology, Cambridge MA 02139, Email: akbarian@mit.edu

[3]George Macomber Professor, Department of Civil & Environmental Engineering, Massachusetts Institute of Technology, Cambridge MA 02139, Email: ulm@mit.edu

ABSTRACT

The dissipation occurring below a moving tire in steady-state conditions in contact with a viscoelastic pavement is expressed using two different reference frames, a fixed observer attached to the pavement, and a moving observer attached to the pavement-tire contact surface. The first approach is commonly referred to as 'dissipation-induced pavement-vehicle-interaction (PVI); the second as 'deflection-induced' PVI. Based on the principle of frame-independence, it is shown that both approaches are strictly equal, from a thermodynamics point of view, and thus predict the same amount of dissipated energy. This equivalence is illustrated through application to two pavement systems, a viscoelastic beam and a viscoelastic plate both resting on an elastic foundation. The amount of dissipated energy in the pavement structure needs to be supplied by the vehicle to maintain constant speed; thus contributing to the rolling resistance, associated excess fuel consumption, and greenhouse

gas emissions. The model here proposed can be used to quantify the dissipated energy, and contribute to the development of engineering methods for the sustainable design of pavements.

Keywords: pavement vehicle interaction, pavement dissipation, viscoelasticity

INTRODUCTION

In his famous book "Viscoelasticity" (Flügge 1967), in conclusion of his analysis of the viscoelastic response of a Kelvin beam on elastic foundation to a moving load, showing that the vehicle load is on an upward slope, Wilhelm Flügge notes that "the load moving with the velocity c has to do work", and that the associated horizontal force "supplies the energy needed for the viscoelastic deformation". He continues that "this phenomenon, well known and occurring in various situations, does not stand in common text books". – The phenomenon has indeed been observed both experimentally and theoretically in many pavement mechanics studies (May et al. (1959), Chupin et al. (2010), Chupin et al. (2013), Greenwood-Engineering (2008), Ferne et al. (2009)); but gained some new attention more recently in the context of the development of engineering methods for the sustainable design of pavements, accounting and eventually reducing the generation of green house gas (GHG) emissions during the use phase of pavements (Akbarian et al. 2012), especially for roads with high traffic volume.

Indeed, in addition to other sources of fuel consumption of road vehicles related to rolling resistance (roughness, friction, and so on; for a review see Beuving et al. (2004)), it has been argued that energy that is dissipated in the process of deforming when subject to a moving load, must be compensated by an external energy source; that is fuel consumption. While there is general agreement on the sources of this mechanically induced additional fuel consumption, there are two schools of thoughts to capture the mechanics of this intriguing phenomenon:

1. Dissipation-induced Pavement Vehicle Interaction (PVI) (Figure 1(a)): The approach

consists in evaluating the energy dissipated in a finite segment of a pavement during the passing time of the vehicle at a constant speed using the (viscoelastic) constitutive behavior of the pavement. This approach pioneered by Pouget et al. (2011), and further refined by Coleri and Harvey (2013), employs finite elements for estimating the time-history of the displacement field in a sufficiently large block of pavement (to minimize the effects of boundary conditions). Using classical finite element procedure stresses and viscoelastic strains are determined.

2. Deflection-Induced Pavement Vehicle Interaction (PVI) (Figure 1(b)): The approach evaluates the dissipation for steady-state conditions of a moving load on a viscoelastic pavement (Chupin et al. 2010 and Chupin et al. 2013). In the vein of Flügge's suggestion (Flügge 1967), it is realized that due to the presence of a dissipative mechanism in the system, the vehicle is always on an uphill slope, leading to an additional horizontal force supplied by the vehicle, that is added to the rolling resistance, and thus to fuel consumption. The approach is implemented by using a semi-analytical method based on wave propagation, via the code "ViscoRoute", in Chabot et al. (2010), and by using the theory of beam on (visco-) elastic foundation in Akbarian et al. (2012).

While on first sight fundamentally different, it is shown in this paper that both approaches are strictly equivalent from a thermodynamic point of view, the sole difference being the reference frame in which the dissipation is expressed. The mathematical proof of the equivalence of these two methods is illustrated through two analytical examples: a viscoelastic Euler-Bernoulli beam and Kirchhoff-Love plate on elastic foundation. By way of example, we also show the implementation of the two approaches for a three-parameter standard linear solid model for the viscoelastic behavior of the pavement.

DISSIPATION RATE

Any objective physics quantity must obey the frame-independence principle. That is, irrespective of the observer's position measuring the physical quantity, the measurement

must be the same. This principle is used below to show that the so-called dissipation-induced PVI and the deflection-induced PVI model are just two ways of measuring the dissipation using two different frames: a fixed frame and a moving frame respectively.

The dissipated energy herein is the one that occurs as a consequence of a tire exerting a surface stress over the tire-pavement contact area onto the pavement. The general definition of the dissipation rate (under isothermal conditions) is given by the Clausius-Duhem inequality, expressing the Second Law of Thermodynamics (see e.g. Coussy 1995, Ulm and Coussy 2002 among many other sources):

$$\mathcal{D} = \delta W - \frac{d\Psi}{dt} \geq 0 \tag{1}$$

where δW is the external work rate supplied to the system, while Ψ is the (Helmholtz) free energy; and d/dt denotes the total time derivative.

Fixed Coordinate System

We first evaluate the dissipation from the point of view of an observer attached to the pavement. The external work rate due to the contact force density (surface traction) supplied from the tire onto the pavement are expressed by surface traction $\underline{T}$ in terms of the Cauchy stress tensor $\underline{\underline{\sigma}}$; i.e. $\underline{T} = \underline{\underline{\sigma}} \cdot \underline{n}$ (with $\underline{n}$ the unit outward normal to the (undeformed) pavement surface S.) Application of the divergence theorem (which cancels out inertia forces) readily yields:

$$\delta W = \int_V \underline{\underline{\sigma}} : \frac{d\underline{\underline{\epsilon}}}{dt}\, dV \tag{2}$$

where $\underline{u}$ is the displacement vector, $\underline{\underline{\epsilon}} = \underline{\underline{\partial u}}$ is the strain tensor and V is the pavement volume. The free energy time derivative, in this non-moving coordinate system, is given by the volume integral:

$$\frac{d\Psi}{dt} = \int_V \frac{d\psi}{dt} dV \tag{3}$$

In the above, ψ is the free energy volume density. Substitution of Eqs. (2) and (3) into (1) readily yields the dissipation rate in the pavement structure (bulk) in the form:

$$\mathcal{D} = \int_V \left(\underline{\underline{\sigma}} : \frac{d\underline{\underline{\epsilon}}}{dt} - \frac{d\psi}{dt} \right) \, dV \geq 0 \tag{4}$$

For pavement materials it is common practice to consider a (linear) viscoelastic constitutive behavior, characterized by the free energy density expression (for a detailed introduction to thermodynamic of viscoelastic behavior, see, for instance, Coussy (1995)):

$$\psi = \frac{1}{2} \left(\underline{\underline{\epsilon}} - \underline{\underline{\epsilon}}^v \right) : \mathbb{C} : \left(\underline{\underline{\epsilon}} - \underline{\underline{\epsilon}}^v \right) + U \left(\underline{\underline{\chi}}^v \right) \tag{5}$$

where $\underline{\underline{\epsilon}}$ is the total strain, $\underline{\underline{\epsilon}}^v$ the viscous strain, $\mathbb{C}$ the forth-order elasticity tensor, while $U(\underline{\underline{\chi}}^v)$ denotes the frozen energy in function of internal state variables $\underline{\underline{\chi}}^v$ that accounts for microelasticity caused by different viscous mechanisms . For instance, for a generalized Kelvin-Voigt model (Figure 2(a)), employed by Pouget et al. (2011) for bituminous mixtures, $\mu = 1, N$ distinct viscous dissipation mechanisms in series, characterized by $\mu = 1, N$ internal variables, $\underline{\underline{\chi}}^v \rightarrow \underline{\underline{\epsilon}}^v_\mu$, contribute to the overall viscous strain $\underline{\underline{\epsilon}}^v = \sum_{\mu=1}^N \underline{\underline{\epsilon}}^v_\mu$, and thus to the dissipation rate $\sum_{\mu=1}^N \underline{\underline{\sigma}}^\mu : d\underline{\underline{\epsilon}}^v_\mu / dt$ (with $\underline{\underline{\sigma}}^\mu = -\partial\psi / \partial \underline{\underline{\epsilon}}^v_\mu = \underline{\underline{\sigma}} - \mathbb{C}^\mu : \underline{\underline{\epsilon}}^v_\mu$); that is:

$$\mathcal{D} = \int_V \sum_{\mu=1}^{N} \left(\sigma^\mu_{ij} \left(\eta^\mu_{ijkl} \right)^{-1} \sigma^\mu_{kl} \right) \, dV \geq 0 \tag{6}$$

where η^μ_{ijkl} are the components of the forth-order viscosity tensor characterizing the viscous strain rate of the μ^{th} viscous dissipative mechanism. Expression (6) still holds for a generalized Maxwell model (Figure 2(b)), in which $\mu = 1, N$ distinct viscous dissipation mechanisms in parallel contribute to the overall stress $\underline{\underline{\sigma}} = \sum_{\mu=1}^N \underline{\underline{\sigma}}^\mu$, if one lets $\underline{\underline{\sigma}}^\mu = -\partial\psi / \partial \underline{\underline{\epsilon}}^v_\mu = \mathbb{C}^\mu : (\underline{\underline{\epsilon}} - \underline{\underline{\epsilon}}^v_\mu)$). In fact, in the absence of a frozen energy that characterizes the free energy of the generalized Maxwell model, the overall viscous strain is $\underline{\underline{\epsilon}}^v = \mathbb{C}^{-1} : \sum_{\mu=1}^N \mathbb{C}^\mu : \underline{\underline{\epsilon}}^v_\mu$, with $\mathbb{C} = \sum_{\mu=1}^N \mathbb{C}^\mu$. Whatever viscoelastic model herein employed, the evaluation of the dissipa-

tion in a fixed coordinate reference frame is at the core of the so-called 'dissipation-induced PVI' approach (Pouget et al. 2011, Coleri and Harvey 2013).

Moving Coordinate System

Consider next an observer attached to the tire-pavement interface ("where the rubber hits the road"), who is moving along the contact area with the tire at a constant speed c, so that the pavement passes by the observer with a velocity $\underline{V}_0 = -c\underline{e}_x$. The moving coordinate system is thus defined by:

$$\underline{X} = \underline{x} - ct\underline{e}_x \tag{7}$$

The time derivative of any function $f(\underline{x}, t)$ obeys the Lagrangian derivative, which for steady-state conditions (where $\partial f(\underline{X}, t)/\partial t = 0$) reads as:

$$\frac{df}{dt} = \underline{V}_0 \cdot \underline{\partial f} \tag{8}$$

where ∂ represents the gradient operator and we note that $\partial_{\underline{x}} = \partial_{\underline{X}}$.

The external work rate provided over the tire–pavement interface recorded by this moving observer is:

$$\delta W = \int_S \underline{V}_0 \cdot \underline{\underline{\partial u}} \cdot \underline{T}\ dS = c \int_S \frac{\partial \underline{u}}{\partial X} \cdot \underline{T}\ \ dS \tag{9}$$

where we made use of $\underline{e}_x \cdot \underline{\underline{\partial u}} = \partial \underline{u}/\partial X$, with $X = x - ct$ defining the position of the observer moving in the $x-$ direction with speed c. Similarly, in this moving coordinate system, the free energy change in the pavement the observer will witness is the free energy that is convectively moving past the observer; and which reads (analogous to the derivation of the $J-$ integral by Rice (1968) in fracture mechanics):

$$\frac{d\Psi}{dt} = \int_{\partial V} \psi \underline{V}_0 \cdot \underline{n}\ da = c \int_{\partial V} \psi n_x\ da \tag{10}$$

where ∂V is the boundary of the pavement volume V (used e.g. in (3)), with outward normal $\underline{n}$. Accordingly, $n_x = \underline{e}_x \cdot \underline{n}$ is the projection of the outward normal onto the driving

direction (cosines director). Hence, the above integral on any (initially) horizontal surface, for which the outward normal is orthogonal to the driving direction is zero. Furthermore, one can always choose the volume V such that its vertical boundaries are far away from the contact area (system choice in thermodynamics), where $\psi = 0$. Thus, under steady-state conditions, the moving observer will not record any change of the free energy. Then it is readily recognized that the dissipation recorded by the moving observer is given by the integral over the tire contact area C:

$$\mathcal{D} = \delta W = c \int_C \frac{\partial \underline{u}}{\partial X} \cdot \underline{T} \ \ dS \geq 0 \tag{11}$$

Note that for an elastic behavior, for which $\mathcal{D} = 0$, thermodynamics defines the possible fields of pressure and displacement distributions. For instance, for a beam and plate on elastic foundation, if the pressure over the contact area is replaced by a concentrated point force $P = -\int_{\mathcal{C}} \underline{e}_z \cdot \underline{T} \ da$, the dissipation rate would read:

$$\mathcal{D} = \delta W = -cP \frac{\partial w}{\partial X} \geq 0 \tag{12}$$

where w is the pavement deflection (positive downward). For the three dimensional media, where slope under a concentrated load is undefined, the dissipation must either be evaluated from the integral in (11) or approximated from:

$$\mathcal{D} = \delta W = -cP \left\langle \frac{\partial w}{\partial X} \right\rangle \geq 0 \tag{13}$$

where $\langle \partial w/\partial X \rangle$ is the average slope along the area of surface load. Hence, for the case of elastic material with no dissipation, the slope is $\partial w/\partial X = 0$, which means that the tire is at the bottom of the deflection basin. However, if dissipation occurs in the pavement structure (for instance, due to viscous deformation mechanisms), the non-negativity of the dissipation (12) requires that $\partial w/\partial X < 0$. This is precisely Flügge's conjecture which he

based on solving the viscoelastic beam problem (Flügge 1967): "Where the load is applied, the beam has an upward slope". Based on the analysis presented here, it turns out that this conjecture is in fact a thermodynamic requirement, required to satisfy the second law of thermodynamics. It is at the core of the so-called 'deflection-induced PVI approach' (Akbarian et al. 2012, Chupin et al. 2010, Chupin et al. 2013).

By way of conclusion, the two schools of thoughts about accounting accurately for the dissipation of energy within a pavement structure due to Pavement-Vehicle Interactions just differ in the chosen reference frame to calculate the same physical quantity: dissipation; that is the amount of mechanical work supplied from the outside that is not stored into the pavement structure; but dissipated into heat form. Since the amount of dissipated energy is independent of the selected reference frame, the dissipation recorded by a fixed observer and by a moving observer must be strictly the same; that is:

$$\mathcal{D} = \int_V \left(\underline{\underline{\sigma}} : \frac{d\underline{\underline{\epsilon}}}{dt} - \frac{d\psi}{dt} \right) \, dV \stackrel{!}{=} c \int_C \frac{\partial \underline{u}}{\partial X} \cdot \underline{T} \;\; da \geq 0 \tag{14}$$

Relation (14) states that any local dissipation within the pavement structure induced by a moving load, is equal to the work rate induced by the stress vector $\underline{T}$ on the tire–pavement interface along the displacement gradient along the driving direction in a moving coordinate system. In what follows, we will illustrate the equivalence of the two approaches for some simplified pavement models, the viscoelastic beam model and the viscoelastic plate model both resting on elastic foundations. The visco-elastic beam and plate are typically used to model different layers of the pavement except for the subgrade, which is represented by the elastic foundation. For illustration only, the approach can be extended to more complex multi-layer models of pavement structures.

VISCOELASTIC EULER-BERNOULLI BEAM ON ELASTIC FOUNDATION

Consider a viscoelastic Euler-Bernoulli beam on an elastic foundation subjected to a vehicle load moving in the $x-$ direction. While the beam-model is certainly the simplest

(and oldest) 1-D representation of stress and strain in a pavement, it serves here to illustrate the thermodynamic result (14). Specifically, for the considered system, there exist a priori two possible thermodynamic systems to be considered:

1. Total System: The thermodynamic system associated with the derivation here above corresponds to the total system, that is beam plus elastic foundation. The external work rate is generated by the stress vector $\underline{T}\ (n) = -p\underline{e}_z$:

$$\delta W = b \int_C p \frac{dw}{dt} dx \tag{15}$$

where C is the tire-pavement contact zone and $w = -\underline{u} \cdot\ \underline{e}_z$ is the vertical displacement (positive downward) of the beam (which within the context of classical beam assumption is equal to the beam deflection; i.e. $u_z = -w$), and b denotes a unit width. The free energy to be considered for this system is the sum of the free energy of beam and elastic foundation, $\Psi = \Psi_B + \Psi_F$. For a linear homogeneous beam element, whose viscous behavior is defined by a Maxwell model, the free energy is conveniently expressed by:

$$\Psi_B = \int_{(\ell)} \psi_S \ dx = \ \frac{1}{2} \int_{(\ell)} \int_S E_0 \left(\epsilon - \epsilon^v\right)^2 dS dx = \frac{1}{2} \int_{(\ell)} E_0 I \left(\chi - \chi^v\right)^2 \ dx \tag{16}$$

where $I = \int_S z^2 dS$, and where we made use of the linearity of the viscous behavior, $\epsilon^v = z\chi^v$, introducing the viscous curvature χ^v. In return, the free energy of the elastic foundation is simply:

$$\Psi_F = b \int_{(\ell)} \frac{kw^2}{2} dx \tag{17}$$

where k is the spring constant. The dissipation is then defined by the Clausius-Duhem inequality (1); which we recall:

$$\mathcal{D} = \delta W - \frac{d}{dt} \left(\Psi_B + \Psi_F\right) \geq 0 \tag{18}$$

2. Beam System: If one isolates the beam from the elastic foundation as the thermodynamic system, the external work rate needs to account for the work generated by a force line density:

$$\underline{f} = f_z \, \underline{e}_z = (-pY + kw) \, b\underline{e}_z \tag{19}$$

where p is the tire pressure, Y is the characteristic function; such that $Y = 1$ in the tire-pavement contact zone C, and $Y = 0$ elsewhere. The external work rate thus generated by f_z reads as:

$$\delta W_B = -\int_{(\ell)} f_z \frac{dw}{dt} \, dx = \delta W - b \int_{(\ell)} kw \frac{dw}{dt} \, dx \tag{20}$$

where δW is given by (15). In return, the free energy to be considered for this system is only the one of the beam, Ψ_B, defined by (16); and the dissipation rate is evaluated from:

$$\mathcal{D} = \delta W_B - \frac{d\Psi_B}{dt} \geq 0 \tag{21}$$

Due to the non-dissipative nature of the support, it is readily understood that expression (18) and (21) must be equal; and hence:

$$\delta W - \delta W_B = \frac{d\Psi_F}{dt} \tag{22}$$

The focus of this section is to develop the dissipation expressions for the two reference frames.

Fixed Coordinate System

We start with the fixed reference frame. We employ as thermodynamic system the isolated beam system. A combination of the beam stress field $\underline{\underline{\sigma}} = \sigma \, \underline{e}_x \otimes \underline{e}_x + \tau \, (\underline{e}_x \otimes \underline{e}_z + \underline{e}_z \otimes \underline{e}_x)$, and the Navier-Bernoulli assumption (axial strain $\epsilon = z\chi$; curvature $\chi =$

$-d^2u_z/dx^2 = d^2w/dx^2$), allows us to develop expression (20) analogous to (2) in the form:

$$\delta W_B = \int_{V_b} \sigma\dot{\epsilon}\ dV = \int_{(\ell)} M\dot{\chi} dx \tag{23}$$

where we used the classical moment–stress relationship, $M = \int_S z\sigma\ dS$. Taking, in the fixed reference frame the time derivative of the beam free energy (16), and subtracting the result from the external work rate (23), the dissipation rate is obtained:

$$\mathcal{D} = \int_{(\ell)} \left(M\dot{\chi} - \frac{d\psi_S}{dt} \right) dx = \int_{(\ell)} M\dot{\chi}^v\ dx \geq 0 \tag{24}$$

together with the state equation for the beam:

$$M = \frac{\partial \psi_S}{\partial \chi} = -\frac{\partial \psi_S}{\partial \chi^v} = E_0 I\left(\chi - \chi^v\right) \tag{25}$$

As expected, we identify the bending moment as the thermodynamic driving force associated in the dissipation (24) to the viscous curvature rate. For a linear viscous behavior of the Maxwell-type, $d\epsilon^v/dt = \sigma/\eta$ (where η is the uniaxial viscosity), this relationship between the thermodynamic force and the associated internal variable rate is readily found to be:

$$\dot{\chi}^v = \frac{1}{\tau}\frac{M}{E_0 I} \tag{26}$$

where $\tau = \eta/E_0$ is the characteristic relaxation time of the Maxwell material. Whence the dissipation rate for the fixed reference frame:

$$\mathcal{D} = \frac{1}{\tau}\int_{(\ell)} \frac{M^2\left(x,t\right)}{E_0 I} dx \geq 0 \tag{27}$$

Moving Reference Frame

Consider now the moving coordinate system $X = x - ct$ attached to the tire-pavement contact surface, which moves with speed c along the beam. For steady-state conditions, the

time derivative follows the Lagrangian derivative, so that with the help of (20) the external work rate in the moving coordinate system for the beam system reads:

$$\delta W_B = c \int_{(\ell)} f_z \frac{dw}{dX}\, dx = -c \int_{(\ell)} M \frac{d\chi}{dX} dX \tag{28}$$

Consider then the constitutive law (26) with (25) in the moving coordinate system:

$$\dot{\chi}^v = -c \frac{d\chi^v}{dX} = -c \frac{d}{dX}\left(\chi - \frac{M}{E_0 I}\right) = \frac{1}{\tau}\frac{M}{E_0 I} \tag{29}$$

A substitution of (29) in (28) yields:

$$\delta W_B = \frac{1}{\tau}\int_{(\ell)} \frac{M^2}{E_0 I} dX - \frac{c}{E_0 I}\int_{(\ell)} M \frac{dM}{dX}\, dX \tag{30}$$

Due to the choice of the beam system as thermodynamic system, we also need to consider the free energy variation of the beam in the moving coordinate system; that is:

$$\frac{d\Psi_B}{dt} = -c \frac{d\Psi_B}{dX} = -c \frac{1}{E_0 I}\int_{(\ell)} M \frac{dM}{dX}\, dX \tag{31}$$

Then, taking the difference between the external work rate and the free energy variation, we readily find:

$$\mathcal{D} = \delta W_B + c \frac{d\Psi_B}{dX} = \frac{1}{\tau}\int_{(\ell)} \frac{M^2(X)}{E_0 I} dX \tag{32}$$

Finally, the comparison of (27) and (32) shows the equivalence of the two approaches. In addition, if we note that in the moving coordinate system the total free energy variation, i.e. of both beam, Ψ_B, and elastic foundation, Ψ_F, is zero (see Eq. (10)), we proof –with the help of (22)– relation (14) for the beam system:

$$\mathcal{D} = \frac{1}{\tau}\int_{(\ell)} \frac{M(x,t)^2}{E_0 I} dx = \frac{1}{\tau}\int_{(\ell)} \frac{M(X)^2}{E_0 I} dX \overset{q.e.d}{\equiv} -cb \int_C p \frac{dw}{dX} dX \geq 0 \tag{33}$$

For purpose of clarity we considered here a Maxwell-beam on an elastic foundation. The principle yet holds for any other linear viscoelastic constitutive behavior of either beam or foundation. For instance, for a beam whose constitutive behavior is described by a Kelvin Chain (the 1-D version of the generalized Kelvin-Voigt model), the proof reads:

$$\mathcal{D} = \int_{(\ell)} \sum_{\mu=1}^{N} \frac{1}{\tau_\mu} \frac{M_\mu^2(x,t)}{E_\mu I} dx = \int_{(\ell)} \sum_{\mu=1}^{N} \frac{1}{\tau_\mu} \frac{M_\mu^2(X)}{E_\mu I} dX \overset{q.e.d}{\equiv} -cb \int_C p \frac{dw}{dX} dX \geq 0 \tag{34}$$

where $\tau_\mu = \eta_\mu / E_\mu$ is the characteristic time of the μ^{th} Kelvin element characterized by a spring of stiffness E_μ in parallel with a dashpot of viscosity η_μ; while the moment M_μ is the thermodynamic force that drives the dissipation $M_\mu \dot{\chi}_\mu^v$:

$$M_\mu = -\frac{\partial \psi_S}{\partial \chi_\mu^v} = M - E_\mu I \chi_\mu^v \tag{35}$$

In the above $M = E_0 I(\chi - \chi^v)$ is the total moment, with $\chi^v = \sum_{\mu=1}^{N} \chi_\mu^v$.

Numerical Results

By way of example, we present here below numerical results for an infinite viscoelastic beam on elastic foundation, the constitutive behavior being described by respectively a Maxwell model (with stiffness E_0 and viscosity η) and a three-parameter standard linear solid model (Kelvin chain with $N = 1(E_1, \eta_1)$). In this numerical approach, the equations of motion of the beam are solved in frequency domain and by using the elastic-viscoelastic correspondence principle.

For the evaluation of the dissipation, we realize from (33) and (34), that the dissipation in a fixed coordinate system can be evaluated from the moments calculated in either fix or moving coordinate system. Since finding the beam response in a moving coordinate system is less computationally expensive, we evaluate the dissipation from (32) for the Maxwell beam;

$$\mathcal{D} = \frac{1}{\tau} \int_{-\infty}^{+\infty} \frac{M(X)^2}{E_0 I} dX \tag{36}$$

and from

$$\mathcal{D} = \frac{1}{\tau_1} \int_{-\infty}^{+\infty} \frac{\left(M - E_1 I \chi^v\right)^2}{E_1 I} dX \tag{37}$$

for the standard linear solid model with $\tau_1 = \eta / E_1$.

To illustrate the numerical solution procedure, we remind us of the equation of motion for an infinite elastic beam on an elastic foundation in a moving coordinate system (Kelly 1962, Frỳba 1999 among many sources):

$$\frac{Eh^3}{12} \frac{\partial^4 w}{\partial X^4} + mc^2 \frac{\partial^2 w}{\partial X^2} + kw = p \tag{38}$$

where m is surface mass density. Taking the Fourier transform of the above equation results in:

$$\widehat{w} = \frac{\widehat{p}}{Eh^3 \lambda^4 / 12 - mc^2 \lambda^2 + k} \tag{39}$$

where λ is the transformed field of X. The inverse Fourier transform of the above gives the elastic solution for a beam on elastic foundation. To evaluate the deflection of a viscoelastic beam, we employ the elastic-viscoelastic correspondence principle (Read 1950, Christensen 1982, Pozhuev 1986), and substitute the complex modulus for its elastic counterpart E in (39). For a Maxwell material with the constitutive equation $\left(\sigma + \tau \dot{\sigma}\right) / E_0 = \tau \dot{\epsilon}$ where $\tau = \eta / E_0$, we have in the moving reference frame, $\left(\sigma - c\tau \ d\sigma / dX\right) / E_0 = -c\tau d\epsilon / dX$. Then, taking the Fourier transformation, i.e. $\hat{\sigma}\left(1 - c\tau \ i\lambda\right) / E_0 = -c\tau i\lambda \hat{\epsilon}$, the complex modulus is obtained:

$$\widehat{E} = -\frac{i\lambda c\tau}{1 - ic\tau\lambda} E_0 \tag{40}$$

Proceeding analogously for a three-parameter solid, the complex modulus reads:

$$\widehat{E} = \frac{\left(1 - i\lambda c\tau_1\right) E_0}{\left(E_0 / E_1 + 1 - i\lambda c\tau_1\right)} \tag{41}$$

where $\tau_1 = \eta_1/E_1$. Substituting $\widehat{E}$ for E in Eq. (39), we obtain for the Maxwell beam:

$$\widehat{w} = \frac{\widehat{p}}{k}\left(\frac{-i\bar{\lambda}\bar{c}\zeta}{1-i\bar{\lambda}\bar{c}\zeta}\bar{\lambda}^4 - \bar{c}^2\bar{\lambda}^2 + 1\right)^{-1} \tag{42}$$

and for the standard linear solid model:

$$\widehat{w} = \frac{\widehat{p}}{k}\left(\frac{E_1/E_0 - i\bar{\lambda}\bar{c}\zeta_1}{1+E_1/E_0 - i\bar{\lambda}\bar{c}\zeta_1}\bar{\lambda}^4 - \bar{c}^2\bar{\lambda}^2 + 1\right)^{-1} \tag{43}$$

where we introduced the following non-dimensional variables:

$$\bar{c} = \frac{c}{c_{cr}}, \quad \bar{\lambda} = L_s\lambda, \quad \zeta = \tau\left(k/m\right)^{1/2}, \quad \zeta_1 = \tau_1\left(k/m\right)^{1/2}\frac{E_1}{E_0} \tag{44}$$

with $L_s = \sqrt[4]{E_0h^3/12k}$ the characteristic Winkler length ($2\pi L_s$ is the width of the deflection basin) and $c_{cr} = L_s\sqrt{k/m}$ is $1/\sqrt{2}$ times the critical (resonant) velocity (Kim and Roesset 2003). Then, if we note that the curvature in Fourier domain is $\widehat{\chi} = -\lambda^2\widehat{w}$, an inverse transformation ($\mathcal{F}^{-1}(\cdot)$) provides the total bending moment:

$$M = \mathcal{F}^{-1}\left(-\lambda^2\widehat{w}\widehat{E}I\right) \tag{45}$$

Expression (45) can be readily employed in (36) to evaluate the dissipation of the Maxwell beam:

$$\mathcal{D} = \frac{1}{\tau}\frac{1}{E_0I}\int_{-\infty}^{+\infty}\left(\mathcal{F}^{-1}\left(-\lambda^2\widehat{w}\widehat{E}I\right)\right)^2 dX \tag{46}$$

In return, for the three-parameter standard linear solid model, the use of (45) in (37) entails:

$$\mathcal{D} = \frac{1}{\tau_1}\frac{1}{E_1I}\int_{-\infty}^{+\infty}\left(\mathcal{F}^{-1}\left(-\lambda^2\widehat{w}\widehat{E}I\right)\left(1+\frac{E_1}{E_0}\right) - E_1I\mathcal{F}^{-1}(-\lambda^2\widehat{w})\right)^2 dX \tag{47}$$

where we used $\chi^v = \chi - M/E_0I = \mathcal{F}^{-1}(-\lambda^2\widehat{w}) - \mathcal{F}^{-1}\left(-\lambda^2\widehat{w}\widehat{E}I\right)/E_0I$.

In return, the dissipation rate in the moving coordinate system is evaluated directly from

the r.h.s. of expressions (33) or (34); that is:

$$\mathcal{D} = -cb \int_C p \frac{dw}{dX} dX = -cb \int_C p \mathcal{F}^{-1}(i\lambda \widehat{w}) dX \tag{48}$$

with $\widehat{w}$ given by (42) for the Maxwell beam, and by (43) for the the three-parameter standard linear solid model. Clearly, from a functional point of view there is no reason that Eqs. (46) or (47) should coincide with expression (48). It is the thermodynamic proof that defines the equality. The dissipation rate is calculated from equations (46)–(48), where the inverse transformations are calculated numerically by Fast Fourier Transform (FFT). The result is shown in Figure 3 in non-dimensional plots for a wide range of vehicle speeds and relaxation time for both the Maxwell and the three-parameter standard linear solid. The results evaluated from the two approaches are close to numerical accuracy in perfect agreement.

VISCOELASTIC KIRCHHOFF-LOVE PLATE ON ELASTIC FOUNDATION

A first refinement of the beam model for pavement structure is the plate model on elastic foundation. Proceeding as for the beam model, we note the difference in the definition of the external work rate supplied to an infinite plate in the (x, y) plane subjected to the pressure action of the tire $\underline{T}\ (n) = -p\underline{e}_z$. The work rate supplied to the total system (plate + elastic foundation) is still given by (2), which can be specified for the plate model in the form:

$$\delta W = \int_C p \frac{dw}{dt} dS \tag{49}$$

where $w(x, y) = -\underline{u} \cdot \underline{e}_z$ is the vertical displacement (positive downward) of the plane (which within the context of classical plate assumption is equal to the plate deflection; i.e. $u_z = -w$). In contrast, isolating the plate from the elastic foundation, the external work rate is due to the tire pressure and the work rate by the elastic spring forces; that is, analogous to (20):

$$\delta W_P = \delta W - \int_{(S)} kw \frac{dw}{dt}\ da \tag{50}$$

With the same reasoning as applied for the beam model, we thus realize that the difference between (49) and (50) is attributable to the change of the free energy Ψ_F of the elastic foundation; that is:

$$\delta W - \delta W_P = \frac{d\Psi_F}{dt} \tag{51}$$

Fixed Coordinate System

We consider the isolated plate system to derive the dissipation expression in the fixed coordinate system. Specifically, we consider a Kirchhoff-Love plate model, for which the in-plane strain components $\underline{\underline{\epsilon}} = (\epsilon_{xx}, \epsilon_{xy}, \epsilon_{yy})$ relate to the second-order curvature tensor $\underline{\underline{\chi}} = -\underline{\underline{\underline{\partial^2 w}}}$:

$$\underline{\underline{\epsilon}} = z\underline{\underline{\chi}} = -z\ \underline{\underline{\underline{\partial^2 w}}};\ \epsilon_{ij} = -z\frac{\partial w}{\partial i \partial j} \tag{52}$$

A substitution of (52) in (2) provides:

$$\delta W_P = \int_{V_p} z\ \underline{\underline{\sigma}} : \dot{\underline{\underline{\chi}}}\ dV = \int_S \underline{\underline{\underline{M}}} : \dot{\underline{\underline{\chi}}}\ da \tag{53}$$

where $\underline{\underline{\underline{M}}} = (M_{xx}, M_{xy}, M_{yy})$ is the (2-D) second-order moment tensor:

$$\underline{\underline{\underline{M}}} = \int_{(h)} -z\ \underline{\underline{\sigma}} dz \tag{54}$$

The free energy of a (homogenous) Maxwell viscoelastic plate can also be written in terms of the curvature tensors:

$$\Psi_P = \int_S \psi_P\ da = \frac{1}{2}\int_S \left(\underline{\underline{\chi}} - \underline{\underline{\chi}}^v\right) : \mathbb{D}_0 : \left(\underline{\underline{\chi}} - \underline{\underline{\chi}}^v\right) da \tag{55}$$

where ψ_P is the the surface free energy density and $\mathbb{D}_0$ is the plate stiffness tensor of components:

$$(D_{ijkl})_0 = D_0 \begin{bmatrix} 1 & \nu & 0 \\ \nu & 1 & 0 \\ 0 & 0 & 1-\nu \end{bmatrix} \tag{56}$$

where $D_0 = E_0 h^3/12\,(1-\nu^2)$ is the (instantaneous) elastic bending stiffness and ν is the Poisson's ratio. The dissipation is then obtained from substituting (53) and (55) in (1):

$$\mathcal{D} = \delta W_P - \frac{d\Psi_P}{dt} = \int_S \underline{\underline{M}} : \dot{\underline{\underline{\chi}}}^v \; da \tag{57}$$

together with the state equation of the Maxwell model:

$$\underline{\underline{M}} = \frac{\partial \psi_P}{\partial \underline{\underline{\chi}}} = -\frac{\partial \psi_P}{\partial \underline{\underline{\chi}}^v} = \mathbb{D}_0 : \left(\underline{\underline{\chi}} - \underline{\underline{\chi}}^v\right) \tag{58}$$

The evolution law for the viscous curvature rate relates the thermodynamic force $\underline{\underline{M}}$ to $\dot{\underline{\underline{\chi}}}^v$; hence for a Maxwell material with constant creep Poisson's ratio is given by:

$$\tau \mathbb{D}_0 : \dot{\underline{\underline{\chi}}}^v = \underline{\underline{M}} \tag{59}$$

where $\tau = \eta/E$ is the relaxation time. Whence the dissipation of the viscoelastic Maxwell plate on an elastic foundation in the fixed coordinate system reads:

$$\mathcal{D} = \frac{1}{\tau} \int_S \underline{\underline{M}}\,(x,y) : \mathbb{D}_0^{-1} : \underline{\underline{M}}\,(x,y) \;\; dx \; dy \tag{60}$$

Moving Coordinate System

In the moving coordinate system $(X = x - ct; Y = y)$, the external work rate of the isolated plate system reads as:

$$\delta W_P = -c \int_S \underline{\underline{M}}\,(X,y) : \frac{d\underline{\underline{\chi}}}{dX}\, dXdy = -c \int_S \underline{\underline{M}}\,(X,y) : \frac{d}{dX}\left(\mathbb{D}_0^{-1} : \underline{\underline{M}} + \underline{\underline{\chi}}^v\right)\, dXdy \tag{61}$$

where we made use of state equation (58). Then, consider the viscous evolution law (59) in this moving frame,

$$-c\tau\mathbb{D}_0 : \frac{d\underline{\underline{\chi}}^v}{dX} = \underline{\underline{M}} \tag{62}$$

A substitution of (62) in (61) yields:

$$\delta W_P = \frac{1}{\tau}\int_S \underline{\underline{M}} : \mathbb{D}_0^{-1} : \underline{\underline{M}}\, dXdy - c\int_S \underline{\underline{M}} : \mathbb{D}_0^{-1} : \frac{d\underline{\underline{M}}}{dX} dXdy \tag{63}$$

Then applying the same reasoning as for the beam model, with the help of (51) we realize that the first term in (63) represents the work rate of the total system (plate and foundation), while the second term is due to the additional work rate provided by the foundation to the isolated plate system. The dissipation in the moving frame is thus expressed by:

$$\mathcal{D} = \delta W_P + c\frac{d\Psi_P}{dX} = \delta W_P - c\frac{d\Psi_F}{dX} = \frac{1}{\tau}\int_S \underline{\underline{M}}\,(X,y) : \mathbb{D}_0^{-1} : \underline{\underline{M}}\,(X,y)\; dXdy \tag{64}$$

Whence, using (49) through (52) the proof for a viscoelastic Maxwell plate is:

$$\mathcal{D} = \frac{1}{\tau}\int_S \underline{\underline{M}}\,(X,y) : \mathbb{D}_0^{-1} : \underline{\underline{M}}\,(X,y)\; dX\; dy \overset{q.e.d}{\equiv} -c\int_C p\frac{dw}{dX} dXdy \geq 0 \tag{65}$$

For the generalize Kelvin-Voigt model (with same Poisson's ratio for all Kelvin units), the proof would read:

$$\mathcal{D} = \int_S \sum_{\mu=1}^{N} \frac{1}{\tau_\mu}\underline{\underline{M}}_\mu\,(X,y) : \mathbb{D}_\mu^{-1} : \underline{\underline{M}}_\mu\,(X,y)\; dX\; dy \overset{q.e.d}{\equiv} -c\int_C p\frac{dw}{dX} dXdy \geq 0 \tag{66}$$

Herein, $\tau_\mu = \eta_\mu / E_\mu$ is the relaxation time of the μ^{th} Kelvin unit, while $\underline{\underline{M}}_\mu$ is the thermodynamic force that drives the rate of viscous curvature:

$$\underline{\underline{M}}_\mu = -\frac{\partial \psi_P}{\partial \underline{\underline{\chi}}^v} = \underline{\underline{M}} - \mathbb{D}_\mu : \underline{\underline{\chi}}^v_\mu = \tau_\mu \mathbb{D}_\mu : \frac{d\underline{\underline{\chi}}^v_\mu}{dt} \tag{67}$$

with $\underline{\underline{M}} = \mathbb{D}_0 : \left(\underline{\underline{\chi}} - \underline{\underline{\chi}}^v\right)$, $\underline{\underline{\chi}}^v = \sum_{\mu=1}^{N} \underline{\underline{\chi}}^v_\mu$, and $\mathbb{D}_\mu = (E_\mu / E_0)\, \mathbb{D}_0$ (for the considered case of a constant creep Poisson's ratio).

Numerical Results

By way of example, consider a viscoelastic plate on elastic foundation. The constitutive behavior of the plate is described by respectively a Maxwell model and a three-parameter standard linear solid model (Kelvin chain with $N = 1$). Proceeding analogous to the beam example, one can use the moments calculated in the moving coordinate system to evaluate the dissipation in a fixed coordinate system. That is, with the help of (66), for a Maxwell plate:

$$\mathcal{D} = \frac{1}{\tau} \int_{-\infty}^{+\infty} \int_{-\infty}^{+\infty} \underline{\underline{M}}\,(X, y) : \mathbb{D}_0^{-1} : \underline{\underline{M}}\,(X, y)\ dX\ dy \tag{68}$$

And for the standard solid plate with $\tau_1 = \eta / E_1$:

$$\mathcal{D} = \frac{1}{\tau_1} \frac{E_0}{E_1} \int_{-\infty}^{+\infty} \int_{-\infty}^{+\infty} \left(\underline{\underline{M}}\,(X, y) - \frac{E_1}{E_0} \mathbb{D}_0 : \underline{\underline{\chi}}^v\right) : \mathbb{D}_0^{-1} : \left(\underline{\underline{M}}\,(X, y) - \frac{E_1}{E_0} \mathbb{D}_0 : \underline{\underline{\chi}}^v\right)\ dX\ dy \tag{69}$$

To illustrate the numerical solution procedure, we recall the equation of motion for an infinite elastic plate on an elastic foundation in a moving coordinate system (Frỳba (1999)):

$$D \left(\frac{\partial^2}{\partial X^2} + \frac{\partial^2}{\partial y^2}\right)^2 w + mc^2 \frac{\partial^2 w}{\partial X^2} + kw = p \tag{70}$$

where $D = Eh^3 / 12\,(1 - \nu^2)$ is the elastic bending stiffness, and m is the mass per unit area

of the plate. Taking the two dimensional Fourier transform of the above equation results in:

$$\widehat{w} = \frac{\hat{p}}{D\left(\lambda_1^2 + \lambda_2^2\right)^2 - mc^2\lambda_1^2 + k} \tag{71}$$

where λ_1 and λ_2 are respectively the transformed fields of X and y. To evaluate the deflection of a viscoelastic plate, using the elastic-viscoelastic correspondence principle, we determine the complex modulus $\widehat{D}$ and substitute for D in (71). For a 3-D creep-behavior characterized by a constant creep Poisson's ratio, the complex modulus is still given by (40) and (41) for the Maxwell model and the three-parameter standard linear solid, so that $\widehat{D} = \widehat{E}h^3/12\,(1-\nu^2)$. Whence, for the Maxwell plate:

$$\widehat{w} = \frac{\widehat{p}}{k}\left(\frac{-i\bar{\lambda}_1\bar{c}\zeta}{1 - i\bar{\lambda}_1\bar{c}\zeta}\left(\bar{\lambda}_1^2 + \bar{\lambda}_2^2\right)^2 - \bar{\lambda}_1^2\bar{c}^2 + 1\right)^{-1} \tag{72}$$

and for the standard linear solid plate:

$$\widehat{w} = \frac{\widehat{p}}{k}\left(\frac{E_1/E_0 - i\bar{\lambda}_1\bar{c}\zeta_1}{1 + E_1/E_0 - i\bar{\lambda}_1\bar{c}\zeta}\left(\bar{\lambda}_1^2 + \bar{\lambda}_2^2\right)^2 - \bar{\lambda}_1^2\bar{c}^2 + 1\right)^{-1} \tag{73}$$

where the non-dimensional variables defined in (44) are used, with $\bar{\lambda}_1 = L_s\lambda_1, \bar{\lambda}_2 = L_s\lambda_2$ and $L_s = \sqrt[4]{D_0/k}$; while $c_{cr} = L_s\sqrt{k/m}$ is $1/\sqrt{2}$ times the critical (resonant) velocity (Kim and Roesset 1998). Then, if we note that the curvature tensor in Fourier domain is $\underline{\underline{\widehat{\chi}}} = (-\lambda_1^2\widehat{w}, -\lambda_2^2\widehat{w}, -\lambda_1\lambda_2\widehat{w})$, a two-dimensional inverse transformation provides the total bending moment:

$$\underline{\underline{M}}\,(X,y) = \mathcal{F}^{-1}\left(\widehat{\mathbb{D}} : \underline{\underline{\widehat{\chi}}}\right) \tag{74}$$

where $\widehat{\mathbb{D}} = \widehat{D}/D_0\ \mathbb{D}_0$ with $\mathbb{D}_0$ given by (56). Expression (74) is readily used in (68) to evaluate the dissipation of the Maxwell plate:

$$\mathcal{D} = \frac{1}{\tau}\int_{-\infty}^{+\infty}\int_{-\infty}^{+\infty} \mathcal{F}^{-1}\left(\widehat{\mathbb{D}} : \underline{\underline{\widehat{\chi}}}\right) : \mathbb{D}_0^{-1} : \mathcal{F}^{-1}\left(\widehat{\mathbb{D}} : \underline{\underline{\widehat{\chi}}}\right)\ dX\ dy \tag{75}$$

For the three-parameter standard linear solid model the dissipation can be evaluated from (69) with:

$$\underline{\underline{M}}\,(X,y) - \frac{E_1}{E_0}\mathbb{D}_0 : \underline{\underline{\chi}}^v = \left(1+\frac{E_1}{E_0}\right)\mathcal{F}^{-1}\left(\widehat{\mathbb{D}} : \underline{\underline{\widehat{\chi}}}\right) - \frac{E_1}{E_0}\mathbb{D}_0 : \mathcal{F}^{-1}(\underline{\underline{\widehat{\chi}}}) \tag{76}$$

where we used $\underline{\underline{\chi}}^v = \underline{\underline{\chi}} - \mathbb{D}_0^{-1} : \underline{\underline{M}} = \mathcal{F}^{-1}(\underline{\underline{\widehat{\chi}}}) - \mathbb{D}_0^{-1} : \mathcal{F}^{-1}\left(\widehat{\mathbb{D}} : \underline{\underline{\widehat{\chi}}}\right)$.

In return, the dissipation rate in the moving coordinate system is evaluated directly from the r.h.s. of expressions (65) or (66); that is:

$$\mathcal{D} = -c\int_C p\frac{dw}{dX}dXdy = -c\int_C p\mathcal{F}^{-1}(i\lambda_1\widehat{w})dXdy \tag{77}$$

with $\widehat{w}$ given by (72) and (73) for the Maxwell plate and the three-parameter standard model, respectively. Again, from a functional point of view, there is no reason that Eqs. (77) and (75) should coincide. They do, however, due to the given proof that the dissipation rate evaluated in two different reference frames is strictly the same. To numerically show the above equivalence, the dissipation rate is calculated from equations (69) and (75)–(77) where the inverse transformations are evaluated using two-dimensional FFT. The results are illustrated in Figure 4 where the non-dimensional dissipation rate is plotted over a wide range of vehicle speeds and relaxation time for both the Maxwell and the three-parameter standard linear plate. The results evaluated from the two approaches perfectly agree close to numerical accuracy.

CONCLUDING REMARKS

The thermodynamic analysis developed in this paper thus reveals that the existing two approaches to accounting for the dissipation as a source of extra-fuel consumption are strictly the same, and differ only in the chosen reference system —fixed vs. moving coordinate frame—; thus confirming Flügge's 1974 conjecture that the upward slope on which a moving load on a viscoelastic beam in steady-state conditions is situated is an added rolling resis-

tance. There are thus different mechanistic means available to quantitatively consider this extra source of fuel consumption related to material deformation in the design of sustainable pavement systems. The model development calls for the following conclusions:

1. Given the (stress, force) linearity of the assumed viscoelastic behavior, the dissipation rate scales with the force magnitude $\mathcal{D} \sim P^2$, and thus with the vehicle or axle load. This is readily depicted from (14) for the continuum system, (33) for the beam system, and (65) for the plate system. However, this scaling may change if any other stress-induced nonlinear mechanism may occur in the system; for instance due to debonding or cracking in the pavement system.
2. A further dimensional analysis of the governing equations allows us to establish a link between the dissipation rate and structural and material properties of the pavement. Specifically, for a Maxwell beam:

$$\Pi = \frac{\mathcal{D} b L_s^2 k}{P^2 c_{cr}} = \mathcal{F}_b \left(\Pi_1 = \frac{c}{c_{cr}}, \Pi_2 = \zeta \right) \tag{78}$$

and the Maxwell plate:

$$\Pi = \frac{\mathcal{D} L_s^3 k}{P^2 c_{cr}} = \mathcal{F}_p \left(\Pi_1 = \frac{c}{c_{cr}}, \Pi_2 = \zeta \right) \tag{79}$$

where the dimensionless function $\mathcal{F}$ depends on the structural system. A close look at Figures 3(a) and 4(a) reveals that the non-dimensional dissipation rate of the beam and plate are constant over the applicable range of vehicle speed. Furthermore, Figures 3(b) and 4(b) show that the non-dimensional dissipation rate is inversely related to ζ and hence the relaxation time. Therefore the scaling relationship can be readily obtained as:

$$\mathcal{D} \propto \tau^{-1} P^2 E^{*-d/4} h^{-3d/4} k^{-1/2+d/4} \tag{80}$$

for both beam and plate models. In the above $d = 1$ and $E^* = E$ for beam model

and $d = 2$ and $E^* = E/(1-\nu^2)$ for plate model.

These scaling relations are in agreement with a recent North American calibration of the World Bank's HDM-4 model for vehicle operating energy costs, $\delta E{=}\mathcal{D}/c$, that reported statistically significant effects of surface texture for heavier trucks ($\delta E{=}\mathcal{D}/c \propto P^2$) and for low speeds ($\delta E \propto c^{-1}$). As such, it is expected that mechanistic-based models of the kind presented here can help to optimize the fuel efficiency of pavement systems. Further studies are required to validate the above scaling relationship which is the subject of ongoing research (Louhghalam et al. 2013). The impact of pavement structural and material properties considered herein needs to be separated from the effect of pavement texture characteristics such as pavement roughness on fuel consumption (Zaabar and Chatti 2010). In fact, roughness leads to dissipation of energy by the vehicle's suspension system; while deflection-induced dissipation, the focus of this paper, results from energy dissipation by deformation mechanisms within the pavement structure. These two sources of energy dissipation need to be separated in the validation. The scaling relations here derived are expected to be useful for this purpose.

ACKNOWLEDGMENT

This research was carried out by the CSHub@MIT with sponsorship provided by the Portland Cement Association (PCA) and the Ready Mixed Concrete (RMC) Research & Education Foundation. The CSHub@MIT is solely responsible for content.

REFERENCES

Akbarian, M., Moeini-Ardakani, S. S., Ulm, F.-J., and Nazzal, M. (2012). "Mechanistic approach to pavement-vehicle interaction and its impact on life-cycle assessment." *Transportation Research Record: Journal of the Transportation Research Board*, 2306(1), 171–179.

506 Beuving, E., De Jonghe, T., Goos, D., Lindahl, T., and Stawiarski, A. (2004). "Fuel efficiency
507 of road pavements." *Proceedings Of The 3rd Eurasphalt and Eurobitume Congress Held*
508 *Vienna, May 2004*, Vol. 1.

509 Chabot, A., Chupin, O., Deloffre, L., and Duhamel, D. (2010). "Viscoroute 2.0 a: Tool for
510 the simulation of moving load effects on asphalt pavement." *Road Materials and Pavement*
511 *Design*, 11(2), 227–250.

512 Christensen, R. (1982). *Theory of viscoelasticity: an introduction*. Academic press.

513 Chupin, O., Piau, J. M., and Chabot, A. (2010). "Effect of bituminous pavement structures
514 on the rolling resistance." *11th International Conference On Asphalt Pavements*.

515 Chupin, O., Piau, J.-M., and Chabot, A. (2013). "Evaluation of the structure-induced rolling
516 resistance (srr) for pavements including viscoelastic material layers." *Materials and Struc-*
517 *tures*, 1–14.

518 Coleri, E. and Harvey, J. T. (2013). "Investigation of layered elastic theory prediction accu-
519 racy for asphalt concrete pavement design using micromechanical viscoelastic finite element
520 modeling." *Materials and Structures*, 1–22.

521 Coussy, O. (1995). *Mechanics of porous continua*. Wiley.

522 Ferne, B. W., Langdale, P., Round, N., and Fairclough, R. (2009). "Development of a cali-
523 bration procedure for the uk highways agency traffic-speed deflectometer." *Transportation*
524 *Research Record: Journal of the Transportation Research Board*, 2093(1), 111–117.

525 Flügge, W. (1967). *Viscoelasticity*. Springer Verlag.

526 Frỳba, L. (1999). *Vibration of solids and structures under moving loads*. Thomas Telford.

527 Greenwood-Engineering (2008). "Traffic speed deflectometer,
528 <www.greenwood.dk/TSD/default.asp>.

529 Kelly, J. M. (1962). *Moving load problems in the theory of viscoelasticity*. Dept. of Civil
530 Engineering.

531 Kim, S.-M. and Roesset, J. M. (1998). "Moving loads on a plate on elastic foundation."
532 *Journal of Engineering Mechanics*, 124(9), 1010–1017.

Kim, S.-M. and Roesset, J. M. (2003). "Dynamic response of a beam on a frequency-independent damped elastic foundation to moving load." *Canadian Journal of Civil Engineering*, 30(2), 460–467.

Louhghalam, A., Akbarian, M., and Ulm, F.-J. (2013). "Scaling relations of dissipation-induced pavement-vehicle interactions." *Transportation Research Record: Journal of the Transportation Research Board*, under review.

May, W., Morris, E., and Atack, D. (1959). "Rolling friction of a hard cylinder over a viscoelastic material." *Journal of Applied Physics*, 30(11), 1713–1724.

Pouget, S., Sauzéat, C., Benedetto, H. D., and Olard, F. (2011). "Viscous energy dissipation in asphalt pavement structures and implication for vehicle fuel consumption." *Journal of Materials in Civil Engineering*, 24(5), 568–576.

Pozhuev, V. (1986). "Steady-state reaction to the effect of a moving load in a system consisting of a cylindrical shell and a viscoelastic filler." *International Applied Mechanics*, 22(5), 415–421.

Read, W. T. (1950). "Stress analysis for compressible viscoelastic materials." *Journal of Applied Physics*, 21(7), 671–674.

Rice, J. (1968). "Fracture: an advanced treatise." *Mathematical Fundamentals*, 2, 191–311.

Ulm, F. and Coussy, O. (2002). *Mechanics and durability of solids: Solid Mechanics, Vol 1.* Prentice Hall.

Zaabar, I. and Chatti, K. (2010). "Calibration of hdm-4 models for estimating the effect of pavement roughness on fuel consumption for us conditions." *Transportation Research Record: Journal of the Transportation Research Board*, 2155(1), 105–116.

LIST OF FIGURES

1. Pavement Vehicle Interaction (PVI) in (a): fixed and (b): moving coordinate systems, (c): moving coordinate system adapted from Flügge 1967
2. Typical visco-elastic models (a): generalized Kelvin-Voigt model, (b): generalized

559 Maxwell model.

560 3. Non-dimensional dissipation rate of an infinite Maxwell and standard linear solid
561 (SLS) beam v.s. (a): non-dimensional velocity c/c_{cr} for $\zeta = \zeta_1 = 1$ and $E_1/E_0 = 1$
562 (b): non-dimensional relaxation time ζ for $c/c_{cr} = 0.2$ and $E_1/E_0 = 1$

563 4. Non-dimensional dissipation rate of an infinite Maxwell and standard linear solid
564 (SLS) plate v.s. (a): non-dimensional velocity c/c_{cr} for $\zeta = \zeta_1 = 1$ and $E_1/E_0 = 1$
565 (b): non-dimensional relaxation time ζ for $c/c_{cr} = 0.2$ and $E_1/E_0 = 1$

List of Figures

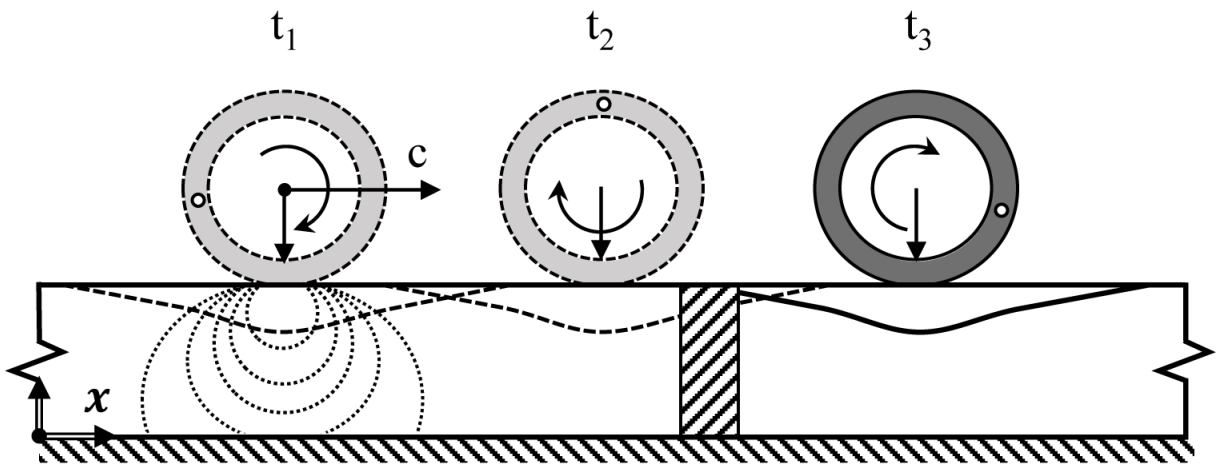

(a)

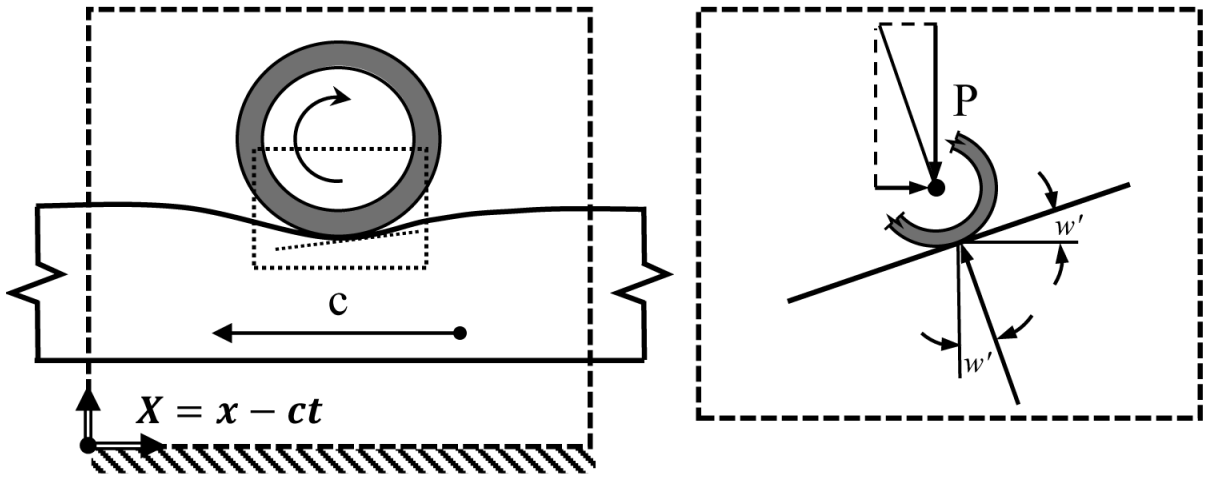

(b) (c)

FIG. 1. Pavement Vehicle Interaction (PVI) in (a): fixed and (b): moving coordinate systems, (c): moving coordinate system adapted from Flügge 1967

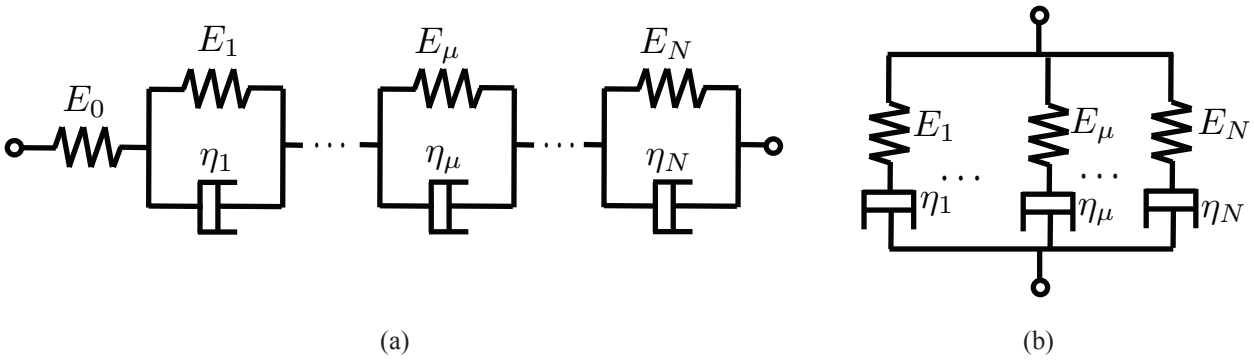

FIG. 2. Typical visco-elastic models (a): generalized Kelvin-Voigt model, (b): generalized Maxwell model.

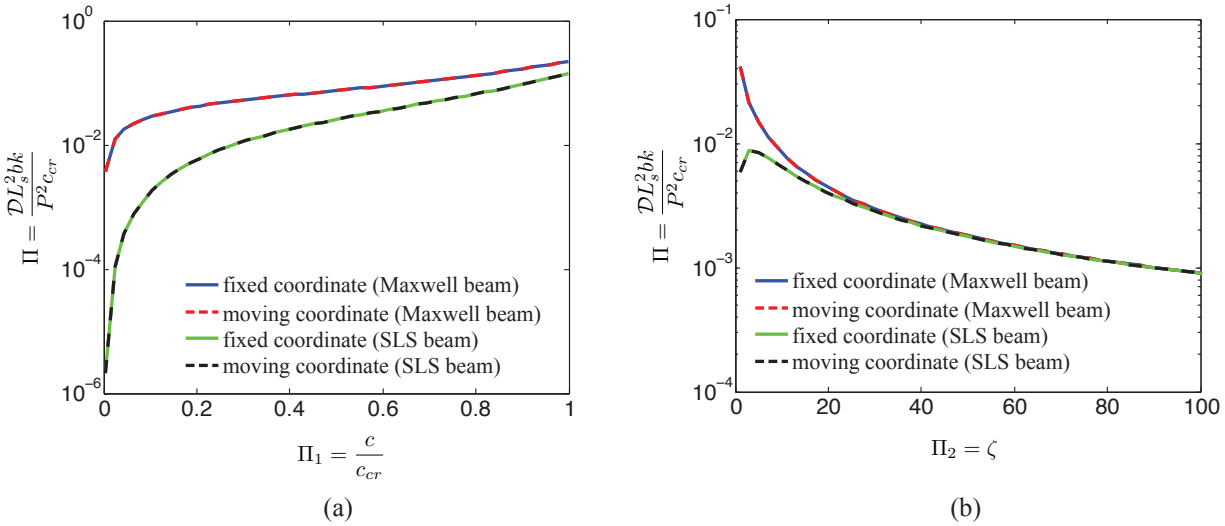

FIG. 3. Non-dimensional dissipation rate of an infinite Maxwell and standard linear solid (SLS) beam v.s. (a): non-dimensional velocity c/c_{cr} for $\zeta = \zeta_1 = 1$ and $E_1/E_0 = 1$ (b): non-dimensional relaxation time ζ for $c/c_{cr} = 0.2$ and $E_1/E_0 = 1$

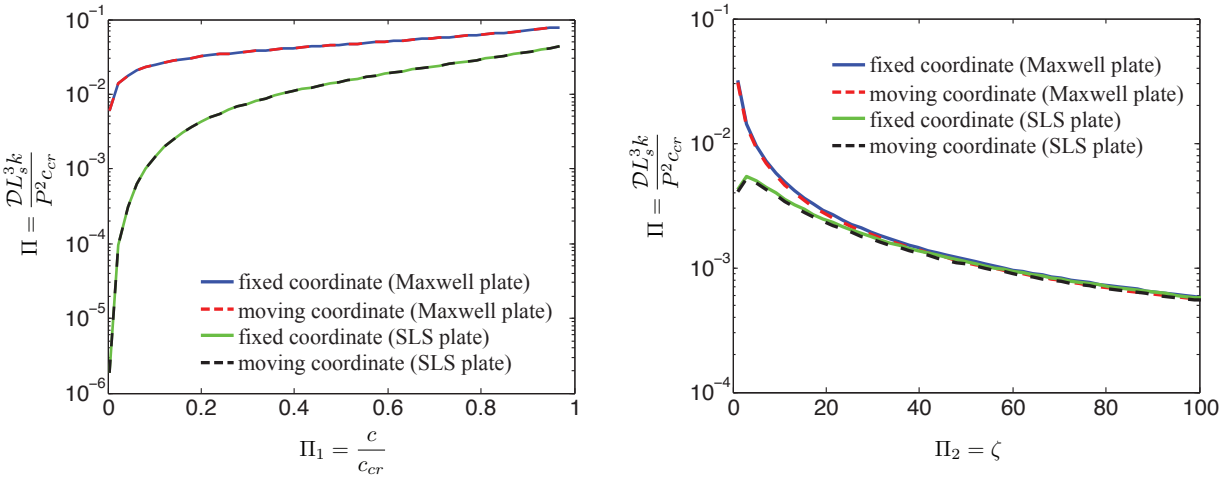

FIG. 4. Non-dimensional dissipation rate of an infinite Maxwell and standard linear solid (SLS) plate v.s. (a): non-dimensional velocity c/c_{cr} for $\zeta = \zeta_1 = 1$ and $E_1/E_0 = 1$ (b): non-dimensional relaxation time ζ for $c/c_{cr} = 0.2$ and $E_1/E_0 = 1$